Pharmaceutical Research, Vol. 22, No. 2, February 2005 (© 2005)
DOI: 10.1007/s11095-004-1189-z

Research Paper

Reversible Lipidization Prolongs the Pharmacological Effect, Plasma Duration, and Liver Retention of Octreotide

Liyun Yuan,[1] Jeff Wang,[2] and Wei-Chiang Shen[1,3]

Received September 26, 2004; accepted November 16, 2004

Purpose. Octreotide (OCT) was reversibly lipidized to improve the pharmacological effect and to increase the plasma half-life and the liver retention of OCT for greater therapeutic potential in the treatment of liver cancers such as hepatocellular carcinoma.
Methods. OCT was chemically modified using reversible aqueous lipidization (REAL) technology. REAL-modified OCT (REAL-OCT) was characterized with high performance liquid chromatography (HPLC) and matrix-assisted laser desorption/ionization time-of-flight (MALDI-TOF) mass spectrometry. A single dose of OCT or REAL-OCT or vehicle only was subcutaneously administered to male Sprague-Dawley rats, and the plasma growth hormone (GH) levels were measured after an intravenous injection of 2.5 μg/kg of growth hormone releasing factor (GRF) to assess the ability of REAL-OCT on GH inhibition. Radio-iodinated Tyr^3-OCT (TOC) and REAL-TOC were used for pharmacokinetic studies.
Results. At 0.1 mg/kg, REAL-OCT inhibited the GRF-induced GH surge in rats for a greater than 24-h period in comparison to the 6-h period for OCT. The distribution and elimination half-life for ^{125}I-REAL-TOC were 1.4 h and 6.6 h, respectively, which were significantly longer than those of ^{125}I-TOC. Sustained high blood concentrations and reduced *in vivo* degradation were observed for ^{125}I-REAL-TOC. In addition, ^{125}I-REAL-TOC appeared to be targeted to the liver with persistent high liver retention.
Conclusions. REAL-OCT has a significantly enhanced pharmacological effect, and this is most likely due to the favorable changes in the pharmacokinetic parameters upon lipidization. The observed liver targeting effect of REAL-TOC suggests that REAL-OCT might be advantageous over OCT in treating liver cancers.

KEY WORDS: growth hormone; liver cancers; liver retention; octreotide; reversible lipidization.

INTRODUCTION

Octreotide (OCT), a long-acting structural derivative of somatostatins, is well established in clinical settings to treat a variety of endocrine disorders such as pituitary and gastroenteropancreatic tumors. OCT is a cyclic octapeptide containing two D-configuration amino acids, with high binding affinity for somatostatin receptor (SSTR) 2 and 5, reduced affinity for SSTR3, and no affinity for SSTR1 and SSTR4 (1). The therapeutic potential of OCT has recently been extended to non-endocrine tumors, particularly primary hepatocelluar carcinoma (HCC) (2). Substantial evidence from experimental studies and clinical trials showed that OCT improved the survival benefits of patients with HCC (3–5). The antineoplastic effects have been attributed to indirect inhibition of insulin-like growth factor-1 (IGF-1) through downregulation of growth hormone (GH) release, direct inhibition of tumor angiogenesis, antiproliferation of tumor cells, and stimulation of the reticuloendothelial system (RES) by unknown mechanisms (2,6,7).

The clinical use of OCT has been limited by the short elimination half-life (less than 2 h), which requires frequent daily subcutaneous (s.c.) or intravenous (i.v.) administration for acute indications or the use of an intramuscular sustained-release formulation for chronic therapy. Its therapeutic potential is also hindered by side effects, including cholesterol gallstones and hyperglycemia upon depression of insulin. Acute administration has also produced receptor desensitization or tolerance. To overcome these limitations, a further modification of OCT is necessary to produce a compound with a prolonged half-life and an optimized biodistribution suitable for specific treatments of diseases such as HCC.

Lipidization is an effective approach to increase the stability of peptides and prolong their half-lives. In general, the carboxylic group of a fatty acid is linked to the amine group of the *N*-terminal residue of a peptide through a stable amide bond. This modification often reduces the affinity of the peptide for receptor binding due to an alteration of its conformation and thus compromises the bioactivities. The lipidized form of somatostatin analogue RC-160 has previously been synthesized with one moiety of myristic acid (14 carbons) coupled to the *N*-terminal residue of RC-160 through a stable amide linkage. When tested *in vitro,* lipidized RC-160 showed

[1] Department of Pharmaceutical Sciences, University of Southern California, Los Angeles, California 90033, USA.
[2] Department of Pharmaceutical Sciences, Western University of Health Sciences, Pomona, California 91766, USA.
[3] To whom correspondence should be addressed. (e-mail: weishen@usc.edu)

increased stability and enhanced antiproliferation (8–10). However, no relevant *in vivo* results have been published so far. Our laboratory has recently developed a reversible aqueous lipidization (REAL) technology for conjugating fatty acid moieties to peptides via reversible disulfide bonds in aqueous solutions, and the disulfide cleavage in the reductive environment *in vivo* release the unmodified therapeutic peptide (11). Therefore, such a modification provides a slow-release delivery system in addition to an increase in lipophilicity. This method has successfully been used for the lipidization of the Bowman-Birk protease inhibitor (12), desmopressin (13), and salmon calcitonin (14). The *in vivo* studies showed that reversible lipidization prolonged the plasma half-lives of these peptides and enhanced their permeation through biological membranes, as well as increased their enzymatic stability. Furthermore, the lipidized peptides had distinct tissue distribution patterns *in vivo*, characterized by high liver uptake and reduced kidney excretion.

In this report, OCT is lipidized using REAL technology. As a result, two moieties of palmitoyl cysteine are coupled to each drug molecule via two reversible disulfide linkages. It is anticipated that OCT will be regenerated slowly from the lipidized derivative, REAL-OCT, upon the cleavage of the disulfide bonds *in vivo* to exert the therapeutic actions. We demonstrate that REAL-OCT acquires many favorable pharmacodynamic and pharmacokinetic properties, including prolonged pharmacological effect, plasma half-life, and liver retention, and may potentially be a better drug for the treatment of HCC.

MATERIALS AND METHODS

Materials

Octreotide (OCT) was purchased from Bachem (Torrance, CA, USA). Tyr^3-OCT (TOC) was synthesized by Genemed Synthesis, Inc (South San Francisco, CA, USA). Human growth hormone releasing factor (1-29) [hGRF(1-29)-NH_2] was obtained from American Peptide Company, Inc. (Sunnyvale, CA, USA). Rat growth hormone (rGH) radioimmunoassay (RIA) kit was purchased from Linco Research, Inc. (St. Charles, MO, USA). Mega bond elut C18 columns were purchased from Varian, Inc. (Palo Alto, CA, USA). Sephadex G25 gel and all other chemicals were obtained from Sigma Chemical Co. (St. Louis, MO, USA). Adult male CF-1 mice aged 6–8 weeks and male Sprague-Dawley rats aged 6–10 weeks were obtained from Charles River Laboratories (Wilmington, MA, USA) and handled in accordance with the Principles of Laboratory Animal Care (NIH Publication No. 85-23, revised 1985). The animals were allowed a standard diet and tap water *ad libitum* and were maintained under controlled conditions (12-h light, 12-h dark schedule; 24°C).

Preparation of REAL-OCT in Dimethylformamide (DMF)

The synthesis of REAL-OCT was slightly modified from the described methods for the synthesis of lipidized desmopressin and lipidized salmon calcitonin (13,14). A solution of 5.0 mg of OCT in 0.9 ml of DMF was mixed with 1.14 mg of dithiothreitol (DTT) in 0.1 ml of DMF at 37°C for 40 min to reduce the disulfide bond between Cys^2 and Cys^7 of OCT. An amount of 10.35 mg *N*-palmitoyl cysteinyl 2-pyridyl disulfide was subsequently added to the solution, and the reaction mixture was stirred for 30 min at 25°C. The mixture was diluted with 10 ml of 50 mM ammonium bicarbonate and loaded on a C18 column. The product was eluted off the column with 90–95% of methanol. The collected fractions were analyzed with high performance liquid chromatography (HPLC) and those containing REAL-OCT were pooled. The solvent was removed by rotary evaporation and 5.6 mg of REAL-OCT was obtained.

Characterization of REAL-OCT

HPLC analysis was conducted on an HP1050 HPLC (Hewlett-Packard, Avondale, PA, USA) system with the wavelength set at 214 nm. A Jupiter C4 column (4.6 × 250 mm; Phenomenex, Torrance, CA, USA) was used and the flow rate was 1 ml/min. The solvents were 10% acetonitrile in 50 mM ammonium bicarbonate, pH 8 (A) and 95% acetonitrile in 50 mM ammonium bicarbonate, pH 8 (B). A gradient program was used starting at 10% of B, increasing to 90% of B in 10 min, and kept at 90% B for additional 10 min.

The samples were also sent to University of Southern California (USC) proteomic core facility for mass determination using matrix-assisted laser desorption/ionization (MALDI) time-of-flight (TOF) analysis. Approximately 10 pmol of the sample in 1 μl DMF was spotted on to a matrix of 10 mg/ml α-cyano-4-hydroxycinnamic acid in 0.1% trifluoroacetic acid/70% acetonitrile and subjected to MALDI-TOF analysis using an Axima-CFR (Kratos Analytical Chestnut Ridge, NY, USA) in reflectron mode following calibration.

The Inhibition of OCT and REAL-OCT on Growth Hormone (GH) Release in Rats

The pharmacological activities of OCT and REAL-OCT were determined by the inhibition of GH release in rats as described previously (15). An amount of REAL-OCT was formulated into 10% Liposyn to reach a final concentration of 0.1 mg/ml. OCT was formulated in the same way. The dose of REAL-OCT described in the following was the OCT-equivalent dose. Male Sprague-Dawley rats weighing 220–280 g (6–10 weeks old) were subcutaneously administered with 0.03 mg/kg of REAL-OCT or OCT. The control received the vehicle only. The rats were then divided into 1-h and 6-h groups and were anesthetized with an intraperitoneal (ip) injection of pentobarbital-sodium (50 mg/kg) 1 h before each time point. Blood samples were collected via the tail tip and the plasma was separated for rGH RIA analysis.

The ability of REAL-OCT on the inhibition of growth hormone releasing factor (GRF) stimulated GH release was also assessed in a similar way described by Bokserand *et al.* (16). Male Sprague-Dawley rats, 4–6 animals per dose, received s.c. injections of REAL-OCT at two different doses (0.03 mg/kg and 0.1 mg/kg). One hour before each time point (1, 6, 24, and 72 h), the rats were anesthetized with pentobarbital-sodium (50 mg/kg, i.p.). Fifty minutes postanesthesia, hGRF(1-29)-NH_2 (2.5 μg/kg) was given intravenously to induce GH release. At 5 min after hGRF injection, blood samples were taken. The plasma GH levels were measured using the rGH RIA kits.

Pharmacokinetic Studies of TOC and REAL-TOC

Synthesis of TOC and REAL-TOC

TOC was used for studying the pharmacokinetic profile because it can be directly labeled with ^{125}I. REAL-TOC was

synthesized and characterized by using the same procedures as described for the preparation and characterization of REAL-OCT. Both TOC and REAL-TOC were iodinated with Na ^{125}I using the chloramine T method (17).

Biodistribution of ^{125}I-TOC and ^{125}I-REAL-TOC After an Intravenous Bolus Injection

Male CF-1 mice aged 6–8 weeks, weighing 22–25 g, were injected intravenously via the lateral tail vein with ^{125}I-TOC or ^{125}I-REAL-TOC at a dose of approximately 1×10^6 cpm per mouse, corresponding to 0.1 mg/kg. Three to four mice were sacrificed each time at 10 min, 30 min, 1 h, 2 h, 4 h, 8 h, and 24 h postinjection (p.i.). The blood samples, as well as the organs of each mouse including lung, liver, spleen, intestines, kidney, pancreas and brain, were collected. The radioactivity in each organ and in 200 μl of blood was measured using a gamma counter (Packard, Downers Grave, IL, USA)

The areas under the concentration-time curves (AUCs) from 10 min to 24 h were calculated by the trapezoidal method for the blood or organs (liver, intestines, colon, and kidneys). The other pharmacokinetic parameters were obtained using a two-compartment model (2COMPK) of the ADAPTII software (D'Argenio DZ & Schumitzky A, USC).

Stability of REAL-TOC

In Vivo Stability of ^{125}I-REAL-TOC

The plasma samples were obtained from mice at 1, 4, and 8 h after the i.v. administration of ^{125}I-TOC and ^{125}I-REAL-TOC. The samples were applied to a Sephadex G-25 size exclusion column (35 ml), eluted with PBS (pH 7.4) containing 0.1% SDS. Fractions (0.5 ml per fraction) were collected and the radioactivity was measured.

In Vitro Stability of ^{125}I-REAL-TOC in Liver Slices and Plasma

Fresh livers were isolated from male CF-1 mice and cut into small slices with a width of 1 mm. ^{125}I-REAL-TOC or ^{125}I-TOC was incubated with 2 g of the liver slices in 15 ml of 5% FBS DMEM medium at 37°C. Aliquots of the incubation medium were taken at 0, 0.5, 1, 2, 4, 8, and 24 h postincubation.

For plasma stability study, blood was collected from male CF-1 mice, and plasma was separated by a brief centrifugation. ^{125}I-REAL-TOC or ^{125}I-TOC was incubated in 1 ml of the plasma at 37°C. Aliquots of the incubation plasma were taken at 0, 0.5, 1, 2, 4, 8, and 24 h postincubation.

The aliquots of the liver or plasma incubation samples were subsequently applied to Sephadex G25 columns (10 ml). Fractions (0.5 ml per fraction) were collected and the radioactivity in each fraction was measured.

Statistical Analysis

One-way ANOVA with Bonferroni adjustment was performed using SPSS 10.0 to determine the level of significance in the data from the animal experiments. Other data were analyzed using an independent Student's *t* test. The data were considered to be statistically significantly different when the p value was less than 0.05.

RESULTS

Characterization of REAL-OCT

Figure 1 shows the structure of REAL-OCT. The cyclic conformation of OCT is disrupted by the reduction of the disulfide bond linking Cys^2 and Cys^7, and the thiol group of each cysteinyl residue is conjugated to one moiety of *N*-palmitoyl cysteine via a disulfide linkage.

REAL-OCT and OCT were analyzed by HPLC under the conditions described in "Materials and Methods." OCT was eluted with a retention time of 8.9 min, whereas REAL-OCT was eluted with a prolonged retention time of 16.1 min. No additional peaks appeared in the HPLC chromatograms, indicating that the purity of REAL-OCT and OCT was over 95%. When REAL-OCT was incubated with 0.1 M DTT at 37°C for 10 min, OCT was released from REAL-OCT, resulting in the shift of the peak from 16.1 min to 8.9 min on HPLC. The mass of REAL-OCT was determined using MALDI-TOF analysis. The measured mass $(M+H)^+$ of REAL-OCT (1736.74 Da) matched the calculated monoisotopic mass (1735.80 Da).

Effect of REAL-OCT on GH Release in Rats

The pharmacological effect of REAL-OCT on GH regulation was assessed in male Sprague-Dawley rats. The GH release was induced following an i.p. injection of pentobarbital sodium in the control group. As shown in Fig. 2, a single s.c. dose of 0.03 mg/kg of either OCT or REAL-OCT inhibited the GH release and maintained a significantly low level of plasma GH at 1 h post drug administration (16 ± 3 ng/ml in OCT; 14 ± 4 ng/ml in REAL-OCT; vs. 229 ± 38 ng/ml in control). The GH inhibition was maintained for more than 6 h in rats treated with REAL-OCT, in comparison to 1 h in rats treated with OCT.

The ability of REAL-OCT to inhibit GRF-stimulated GH release was also measured. The control group showed a marked increase of GH release 5 min following an i.v. injection of hGRF, and the GH surges ranging from 1200 to 1600 ng/ml were reproducible when the rats were treated repeatedly with hGRF at 1, 6, 24, and 72 h. The GH surge was

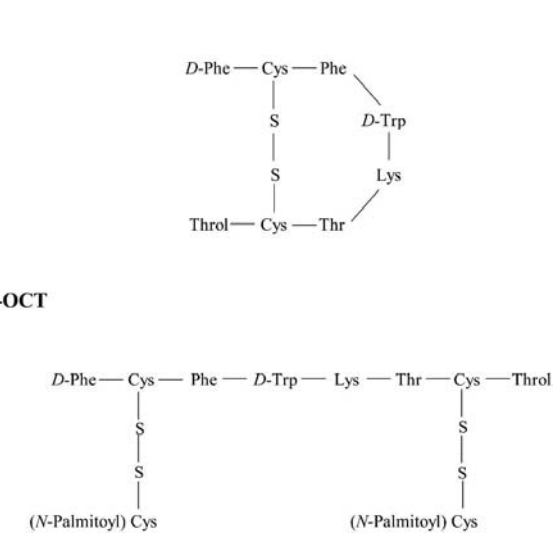

Fig. 1. Structures of OCT (A) and REAL-OCT (B).

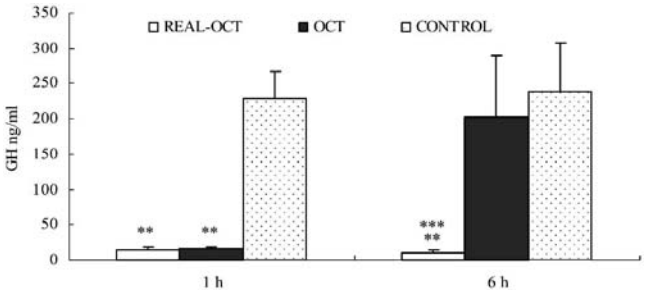

Fig. 2. The inhibitory effects of REAL-OCT and OCT on pentobarbital sodium–induced GH secretion in rats. REAL-OCT or OCT or vehicle (as control) was injected s.c. to male Sprague-Dawley rats at a single dose of 0.03 mg/kg. GH secretion was induced 60 min after i.p. injection of pentobarbital sodium (50 mg/kg) and plasma GH levels were measured using a rGH RIA kit. Inhibition of GH release was determined at 1 and 6 h post drug administration. **$p < 0.001$ (vs. control); ***$p < 0.001$ (vs. OCT). Data are mean ± SD (n = 4–6).

significantly suppressed for more than 24 h in rats treated with REAL-OCT at a single s.c. dose of 0.1 mg/kg. However, the suppression of GH surges lasted for only 6 h in rats treated with OCT at the same dose (Fig. 3).

The pharmacological effect of REAL-OCT was dose-dependent. With a lower dose, REAL-OCT had a shorter duration of action in inhibition of GRF-stimulated GH release. Compared to the dose of 0.1 mg/kg that lasted for 24 h, the dose of 0.03 mg/kg maintained the GH inhibition for 6 h (Fig. 4).

Pharmacokinetic Profile

Blood Concentration vs. Time Course of ^{125}I-REAL-TOC

The analogue TOC, which has a single substitution of Phe^3 in OCT by Tyr^3 as a radioiodination site, was used for the pharmacokinetic studies. TOC was biologically active in inhibiting GH release when administered subcutaneously to rats (data not shown). REAL-TOC was synthesized and characterized with the same procedures as described for REAL-OCT in "Materials and Methods." By using MALDI-TOF mass spectrometric analysis, the signal of the protonated REAL-TOC was found to be 1752.31 Da, which was consistent with the calculated monoisotopic mass of REAL-TOC itself (1751.80 Da). Figure 5 shows the blood level vs. time profiles following a single i.v. bolus administration. The C_{max} of ^{125}I-REAL-TOC (17.65% ID/ml) was reached at 30 min p.i. and declined to 4.24% ID/ml in the blood at 4 h p.i. In contrast, the C_{max} of ^{125}I-TOC in the blood was 4.22% ID/ml at 10 min p.i. and declined quickly to 0.51% ID/ml at 4 h p.i.. The blood concentration of ^{125}I-REAL-TOC at each observed time point was significantly higher than that of ^{125}I-TOC, leading to the 7.9-fold higher AUC. This evidence provides a direct explanation for the prolonged effect of REAL-OCT observed in rats as accounted by measuring GH inhibition.

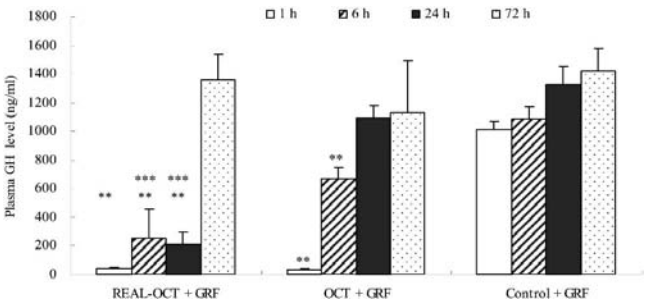

Fig. 3. Inhibition of REAL-OCT on GRF-stimulated GH release in anesthetized rats. REAL-OCT or OCT or vehicle (as control) was injected s.c. to male Sprague-Dawley rats at a single dose of 0.1 mg/kg. The rats were then anesthetized via i.p. injection of pentobarbital sodium. Fifty minutes after anesthesia, GH surges were induced 5 min after i.v. injection of hGRF-NH_2 (2.5 μg/kg). Inhibition of GH surges was determined at 1, 6, 24, and 72 h postadministration of OCT or REAL-OCT. **$p < 0.001$ (vs. control); ***$p < 0.001$ (vs. OCT). Data are mean ± SD (n = 4–6).

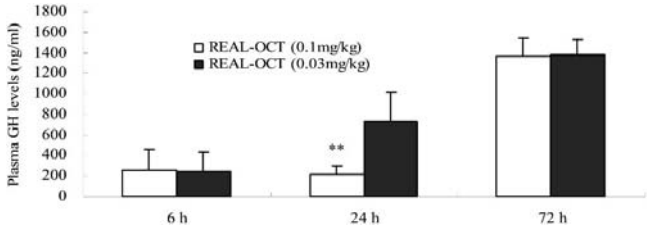

Fig. 4. Dose-dependent GH inhibition of REAL-OCT in Sprague-Dawley rats. Two doses of REAL-OCT, 0.03 mg/kg and 0.1 mg/kg, were injected s.c. Inhibition of GRF-stimulated GH secretion was compared at 6, 24, and 72 h post drug application. **$p < 0.001$ (vs. 0.03 mg/kg). Data are mean ± SD (n = 4–6).

Pharmacokinetic parameters of TOC and REAL-TOC were generated using a two-compartment model, 2COMPK, within the ADPT II program. As listed in Table I, the distribution and elimination half-life for ^{125}I-REAL-TOC were 1.4 h and 6.6 h, respectively. The total plasma clearance (CL_T) of ^{125}I-REAL-TOC (1.7 ml/h) is lower than that of ^{125}I-TOC (13.1 ml/h).

Tissue Distribution of ^{125}I-TOC and ^{125}I-REAL-TOC

The tissue distribution of ^{125}I-TOC and ^{125}I-REAL-TOC in male CF-1 mice at 10 min, 30 min, 1 h, 2 h, 4 h, 8 h, and 24 h were compared (Table II). Both radioiodinated peptides were excreted via the hepatobiliary system. Following an initial uptake in the liver, ^{125}I-TOC was rapidly cleared, resulting in a surge of radioactivity in the intestines with the maxi-

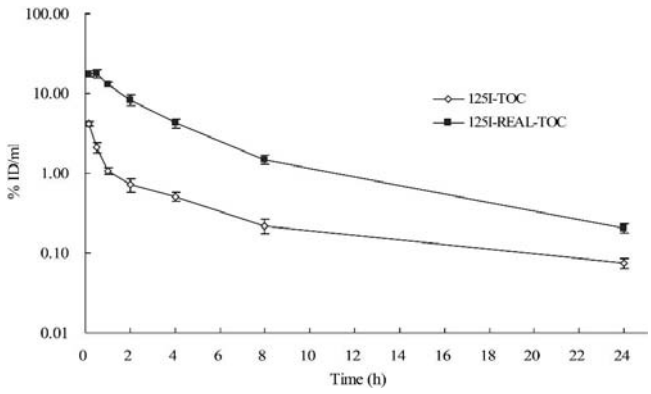

Fig. 5. The blood concentration vs. time profiles following an i.v. bolus administration of ^{125}I-TOC or ^{125}I-REAL-TOC to CF-1 male mice. Three to four mice were sacrificed at each time point and the radioactivity in 200 μl of blood was measured. Each data point represents the mean value ± SD of 3–4 mice, with the unit of percentage of the injected dose per ml of blood (% ID/ml).

Table I. Relevant Pharmacokinetic Parameters of ^{125}I-TOC and ^{125}I-REAL-TOC

	^{125}I-TOC	^{125}I-REAL-TOC
Vc (ml)	15.6	5.0
CL_T (ml/h)	13.1	1.7
α	3.0	0.5
β	0.2	0.1
t1/2-α (h)	0.2	1.4
t1/2-β (h)	4.2	6.6

^{125}I-REAL-TOC and ^{125}I-TOC were administered intravenously at a dose of approximately 1×10^6 cpm per mouse, corresponding to 0.1 mg/kg. The pharmacokinetic parameters were obtained by analyzing the blood concentrations vs. time profile using a two-compartment model (2COMPK) of the ADAPTII software.
CL_T: total body clearance; α: distribution rate constant; β: elimination rate constant; t1/2-α: the half-life of the distribution phase; t1/2-β: the half-life of the elimination phase.

mum of 31.99 ± 2.39% ID/g at 1h p.i. and a maximum of 29.31 ± 1.32% ID/g at 2 h p.i. in the colon. In contrast, the concentration of ^{125}I-REAL-TOC in the intestines was slowly increased to a maximum of 8.35 ± 1.05% ID/g at 2 h p.i. Both labeled peptides were also excreted via the kidneys; however, kidney uptake of ^{125}I-REAL-TOC was significantly lower than that of ^{125}I-TOC. The distribution in the pancreas and the brain was very low and comparable for both peptides at all time points (data not shown in Table II).

The tissue distribution of ^{125}I-REAL-TOC was primarily distinguished with high liver and spleen uptake. Following a high liver uptake at 10 min pi (24.17 ± 5.11% ID/g), ^{125}I-REAL-TOC concentration in the liver reached a plateau at 2 h p.i. and declined to 5.80% ID/g at 24 h p.i. The initial liver uptake of ^{125}I-TOC was comparable to that of ^{125}I-REAL-TOC, with a value of 19.29% ID/g at 10 min p.i. However, ^{125}I-TOC was rapidly excreted through the hepatobiliary system and its concentration reduced to 1.87% ID/g in the liver at 24 h p.i. As a result, AUC of ^{125}I-REAL-TOC was 3.8-fold higher than that for ^{125}I-TOC in the liver. The spleen accumulation of ^{125}I-REAL-TOC was also striking. When compared to that of ^{125}I-TOC, the concentration of ^{125}I-REAL-TOC in the spleen was increased by a factor of 9- to 10-fold at almost all observed time points, leading to a 7-fold higher AUC. However, the amount of ^{125}I-REAL-TOC in the spleen was much lower than that in the liver, that is, 12.47 ± 2.77 vs. 24.21 ± 1.49 ID/g at 1 h p.i., respectively.

Stability of REAL-TOC

In Vivo Degradation of ^{125}I-TOC and ^{125}I-REAL-TOC

The plasma was collected at 1, 4, and 8 h post i.v. injection of ^{125}I-REAL-TOC or ^{125}I-TOC to mice and was applied to a Sephadex G25 column. The peak in the void volume represented the intact peptide, including the plasma protein-bound form and the free form. The small degradation products, unbound to proteins, were eluted as the later peaks (Fig. 6). ^{125}I-REAL-TOC was highly stable *in vivo* and thus only a very small amount of degradation products was detected in the plasma at 8 h p.i. On the other hand, ^{125}I-TOC was relatively unstable and almost 50% of the injected dose was degraded within 4 h. The plasma radioactivity of ^{125}I-TOC at 8 h p.i. was too low to be detectable by this assay method.

In Vitro Stability of ^{125}I-TOC and ^{125}I-REAL-TOC in Liver Slices and Plasma

The stability of TOC and REAL-TOC in mouse liver slices and plasma were measured using Sephadex G25 columns. Both ^{125}I-TOC and ^{125}I-REAL-TOC are relatively stable in plasma, with less than 10% being degraded during the 24-h incubation (Fig. 7A). When incubated with liver slices for 24 h, ^{125}I-REAL-TOC showed to be more stable than ^{125}I-TOC, and only 30% of ^{125}I-REAL-TOC was extensively degraded, as compared to 61% of ^{125}I-TOC (Fig. 7B).

DISCUSSION

In this report, we conjugated two moieties of palmitoyl cysteine to cys^2 and cys^7 of OCT and TOC via reversible disulfide bonds to form REAL-OCT and REAL-TOC. When administered to Sprague-Dawley rats, REAL-OCT inhibited pentobarbital sodium-induced GH secretion and GRF-stimulated GH secretion, a similar effect as reported for OCT and other OCT analogs (16,18). However, the inhibition of GH release by REAL-OCT lasted for over 24 h when a single sc dose of 0.1 mg/kg was used, whereas the effect of OCT lasted only 6 h at the same dose. These results clearly prove the protracted activity of REAL-OCT. As shown in Fig. 1, the lipidization of OCT involves the conversion of the cyclic conformation to a linear one. Because the linear conformation is less favorable for affinity and selectivity of the native peptides or analogues to the somatostatin receptors (19), the release of the lipids and subsequent regeneration of the disulfide bond between Cys^2 and Cys^7 to form the cyclic conformation likely occurred *in vivo* to exert biological activity. OCT regeneration was achieved after incubation of REAL-OCT with the reducing agent DTT *in vitro*. Our previous reports also demonstrated that sustained levels of original peptides were regenerated from REAL-peptides *in vivo* (12,13).

Further investigation of the plasma half-life and biodistribution of REAL-OCT as compared to OCT was performed. However, the lack of a tyrosyl residue in OCT prohibits direct radiolabeling of this peptide. Therefore, an OCT analogue, TOC, was used instead for the pharmacokinetic investigation. TOC has a close chemical structure and molecular size to OCT. More importantly, TOC maintains comparable affinity and selectivity with that of OCT for the SSTR2, 3, and 5 receptors (20). ^{123}I-TOC has previously been evaluated as a potential radiotracer for targeted imaging and radiotherapy of SSTR2-positive tumors (21,22). We also demonstrated that TOC, like OCT, was active in inhibiting GH release when administered in rats (data not shown). Based on the above considerations, we reasoned that the pharmacokinetics pattern of TOC would be comparable to that of OCT.

As expected, the blood levels of ^{125}I-REAL-TOC were significantly higher than those of ^{125}I-TOC at each time point, leading to the 7.9-fold higher AUC. This is consistent with the prolonged pharmacological effect of REAL-OCT. Using a two-compartment model, the distribution half-life of REAL-TOC was 1.4 h, which was significantly longer than 13 min for TOC. The slow distribution phase is likely due to the slow release of TOC from the conjugate, which subsequently binds to or is internalized into the tissues. The high affinity of REAL-OCT for plasma proteins may also contribute to the slow absorption. Although the elimination half-life of REAL-

Table II. Tissue Distribution of Intravenously Injected ^{125}I-REAL-TOC and ^{125}I-TOC in CF-1 mice

	10 min	30 min	1 h	2 h	4 h	8 h	24 h
Lung[a]	7.75 ± 0.08	5.97 ± 0.51	4.58 ± 0.70	3.49 ± 1.06	2.56 ± 0.49	1.28 ± 0.15	0.57 ± 0.12
	4.85 ± 0.78	2.67 ± 0.22	2.14 ± 0.12	1.84 ± 0.25	1.64 ± 0.24	1.51 ± 0.12	0.77 ± 0.09
Liver[a]	24.17 ± 5.11	22.99 ± 0.32	24.21 ± 1.49	20.49 ± 4.54	15.51 ± 3.15	11.25 ± 0.47	5.80 ± 0.74
	19.29 ± 1.17	13.46 ± 2.01	10.35 ± 1.05	5.33 ± 0.72	2.60 ± 0.29	2.21 ± 0.15	1.87 ± 0.30
Intestine[a]	1.80 ± 0.48	3.94 ± 0.23	6.17 ± 0.49	8.35 ± 1.05	6.11 ± 0.98	1.79 ± 0.19	0.38 ± 0.05
	10.84 ± 2.60	25.55 ± 1.67	31.99 ± 2.39	8.89 ± 3.29	1.47 ± 0.30	0.52 ± 0.09	0.16 ± 0.02
Colon[a]	0.32 ± 0.12	0.41 ± 0.09	0.48 ± 0.10	1.82 ± 1.54	7.69 ± 1.03	2.83 ± 0.38	0.57 ± 0.17
	0.40 ± 0.02	0.25 ± 0.03	0.29 ± 0.06	29.31 ± 1.32	10.83 ± 5.46	1.60 ± 0.73	0.24 ± 0.06
Spleen[a]	14.61 ± 1.97	14.61 ± 4.88	12.47 ± 2.77	9.67 ± 2.34	6.23 ± 1.76	4.35 ± 1.40	1.22 ± 0.24
	1.48 ± 0.08	1.65 ± 0.12	1.22 ± 0.09	0.92 ± 0.11	0.62 ± 0.06	0.47 ± 0.10	0.66 ± 0.22
Kidney[a]	3.85 ± 0.66	5.34 ± 0.56	4.26 ± 0.40	3.42 ± 0.81	3.22 ± 0.60	1.77 ± 0.14	0.71 ± 0.10
	10.20 ± 1.47	8.47 ± 0.43	9.00 ± 0.97	6.38 ± 0.61	3.76 ± 0.29	2.70 ± 0.16	1.15 ± 0.14

Data are presented as mean values ± SD (n = 3 to 4), with the unit of percentage of injected dose per gram of tissue (% ID/g).
[a] Top rows of data are the values of ^{125}I-REAL-TOC; bottom rows of data are the values of ^{125}I-TOC.

TOC was only slightly extended to 6.6 h, the C_{max} of REAL-TOC was significantly higher. To ascertain whether the total blood radioactivity used in determining the pharmacokinetic parameters reflected intact peptides or metabolites, the portion of intact peptides in the blood at 1 h, 4 h, and 8 h p.i. was measured. Almost half of ^{125}I-TOC was degraded within 4 h post i.v. injection, whereas little degradation was observed for ^{125}I-REAL-TOC. Considering the blood concentration of the intact peptide vs. time profile, the elimination half-life of TOC would actually be much shorter than 4 h, whereas the elimination half-life of REAL-TOC would remain at approximately 6.6 h.

The *in vitro* stability of REAL-TOC and TOC were also determined. Both peptides were relatively stable in mouse plasma. In liver slice incubation, about 20% of TOC was degraded within 4 h while 12% of REAL-TOC underwent metabolism. It seems that the *in vitro* liver metabolism is not extensive enough to account for the degradation of TOC (about 50%) that was observed *in vivo*. The degradation of TOC may occur in some tissues other than the liver. It is also possible that TOC is extensively degraded in the GI tract

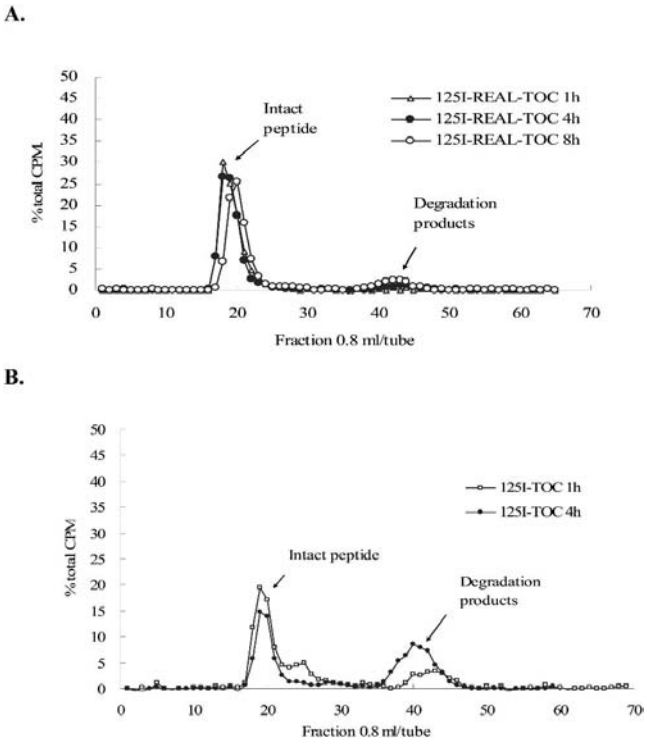

Fig. 6. Stability of ^{125}I-REAL-TOC (A) and ^{125}I-TOC (B) *in vivo*. The plasma samples were obtained at 1, 4, and 8 h post i.v. injection of ^{125}I-REAL-TOC or ^{125}I-TOC to male CF-1 mice. Drug degradation in the plasma was measured using a Sephadex G25 column (35 ml) as described in "Materials and Methods." (In the case of ^{125}I-TOC, the total radioactivity at 8 h was too low to be detectable.)

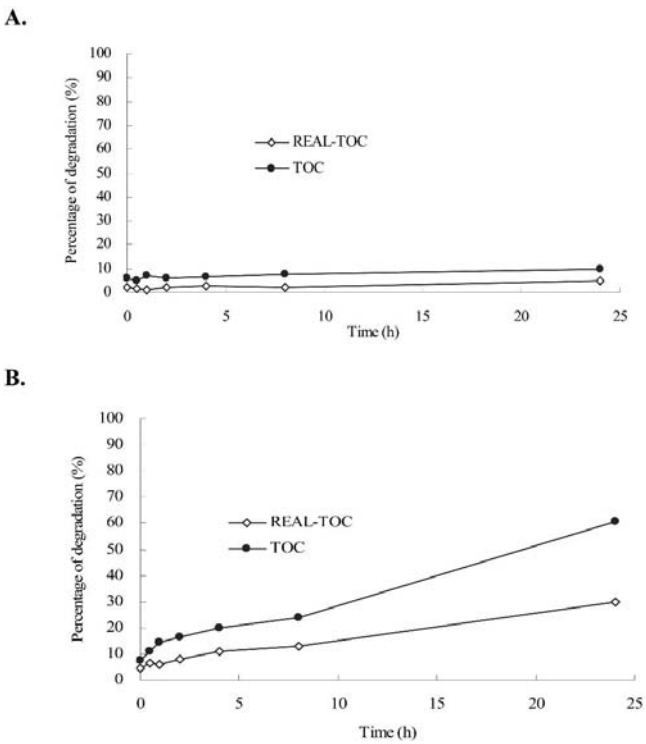

Fig. 7. The metabolic stability of ^{125}I-REAL-TOC and ^{125}I-TOC in mouse plasma (A) and mouse liver slices (B). The compounds were incubated in mouse plasma or liver slices at 37°C. Aliquots at 0, 0.5, 1, 2, 4, 8, or 24 h postincubation were taken, and drug degradation in the aliquots was measured using a Sephadex G25 column (10 ml).

following the bililary excretion, and the small TOC metabolites may be reabsorbed into the blood via the enterohepatic circulation, which partially contribute to the total degradation determined *in vivo*.

The tissue distribution of REAL-TOC was primarily characterized by a high liver retention and spleen uptake. High liver uptake and rapid biliary excretion was found in most of the somatostatin analogues and contributed to their short plasma half-lives. In a study where (^{3}H or ^{14}C) OCT was administered intravenously to rats, 90% of the biliary excretion occurred within the first 2 h and accounted for about 50% of the injected dose (23). Here, a similar pattern was observed with TOC: following a peak concentration in the liver within 10 min, ^{125}I-TOC was quickly eliminated into the intestines. Lipidization increased the initial uptake even more with 24.17% ID/g of REAL-TOC distributed into the liver. This could be due to tight and nonspecific binding to liver tissue proteins, promoted by lipid moieties in the conjugate. Nevertheless, high liver concentration of REAL-TOC persisted with slow elimination into the small intestine. As a result, an overall liver retention of REAL-TOC was observed for 24 h. The biliary excretion of somatostatin analogues is known to involve an active transport system in the bile canalicular membrane of hepatocytes. Although the associated transporters have not been characterized, charge and hydrophobicity of the substrates was found to affect the transport (24,25). The increased hydrophobicity and overall neutral form of REAL-TOC seems to be less favored by the transporters than cationic TOC. Alternatively, lipidization may alter intrahepatic distribution, resulting in lower uptake by hepatocytes. Many studies have shown that the reticuloendothelial tissue favors large lipophilic molecules and/or lipid formulations, such as lipiodol and liposomes (26). This phenomenon has been applied to develop drug conjugates targeting Kupffer cells in the liver. One of the many examples is the lipophilic glyceroyl dipalmitate derivative of muramyl dipeptide (MDP). The lipidized MDP formulated in liposomes was more effective in the activation of macrophages than MDP, and this system successfully induced the tumoricidal activity of Kupffer cells in murine liver metastasis models (27). Similarly, the REAL technology converts TOC into a larger lipophilic molecule that can be subsequently incorporated into the Liposyn formulation. The lipophilic peptide, together with the lipid formulation, likely enhances the uptake by Kupffer cells rather than by hepatocytes. In support of this hypothesis, REAL-TOC was also observed at profoundly high levels in the spleen, the biggest lymphatic organ rich in reticuloendothelial cells where the lipid-like conjugate is likely to be internalized.

CONCLUSIONS

Our data demonstrate that the lipidized derivative of OCT, REAL-OCT, has a long duration of action for inhibition of GH release in anesthetized rats. This is consistent with the observed prolonged plasma half-life and sustained high C_{max} in the blood. Therefore, to achieve the same therapeutic effect of OCT, REAL-OCT may need less frequent administrations with a lower dose. More interestingly, there was high liver and spleen retention of the lipidized drug and when formulated into Liposyn, REAL-OCT seems to be targeted to RES in these organs. Because OCT has a clear stimulatory effect on the hepatic and splenic RES activity, and this action was postulated to be important in the inhibition of liver tumor growth and development (28–30), therefore, REAL-OCT, combined with its high potency in GH inhibition (GH/IGF axis), may be more potent in the treatment of HCC and liver metastasis.

ACKNOWLEDGMENTS

The authors acknowledge the excellent technical support from Daisy Shen. This work was supported in part by a contract from Pharmdel, Inc.

REFERENCES

1. S. W. Lamberts, A. J. van der Lely, W. W. de Herder, and L. J. Hofland. Octreotide. *N. Engl. J. Med.* **334**:246–254 (1996).
2. E. A. Kouroumalis. Octreotide for cancer of the liver and biliary tree. *Chemotherapy* **47**:150–161 (2001).
3. D. N. Samonakis, J. Moschandreas, T. Arnaoutis, P. Skordilis, C. Leontidis, I. Vafiades, and E. Kouroumalis. Treatment of hepatocellular carcinoma with long acting somatostatin analogues. *Oncol. Rep.* **9**:903–907 (2002).
4. M. Raderer, M. H. Hejna, C. Muller, G. V. Kornek, A. Kurtaran, I. Virgolini, W. Fiebieger, G. Hamilton, and W. Scheithauer. Treatment of hepatocellular cancer with the long acting somatostatin analog lanreotide in vitro and in vivo. *Int. J. Oncol.* **16**: 1197–1201 (2000).
5. J. T. Siveke, C. Folwaczny, and C. Herberhold. Complete regression of advanced HCC with long acting octreotide. *Gut* **52**:1531 (2003).
6. C. Scarpignato and I. Pelosini. Somatostatin analogs for cancer treatment and diagnosis: an overview. *Chemotherapy* **47**:1–29 (2001).
7. C. Bousquet, E. Puente, L. Buscail, N. Vaysse, and C. Susini. Antiproliferative effect of somatostatin and analogs. *Chemotherapy* **47**:30–39 (2001).
8. P. Dasgupta, A. Singh, and R. Mukherjee. N-terminal acylation of somatostatin analog with long chain fatty acids enhances its stability and anti-proliferative activity in human breast adenocarcinoma cells. *Biol. Pharm. Bull.* **25**:29–36 (2002).
9. P. Dasgupta, A. T. Singh, and R. Mukherjee. Lipophilization of somatostatin analog RC-160 improves its bioactivity and stability. *Pharm. Res.* **16**:1047–1053 (1999).
10. P. Dasgupta, A. T. Singh, and R. Mukherjee. Lipophilization of somatostatin analog RC-160 with long chain fatty acid improves its anti-proliferative activity on human oral carcinoma cells in vitro. *Life Sci.* **66**:1557–1570 (2000).
11. W. C. Shen, J. Wang, and D. Shen. Reversible lipidization for the delivery of peptide and protein drugs. In S. Frøkjær, L. Christrup, and P. Krogsgaard-Larsen (eds.), *Peptide and Protein Drug Delivery*, Munksgaard, Copenhagen, 1998, pp. 397–408.
12. L. Honeycutt, J. Wang, H. Ekrami, and W. C. Shen. Comparison of pharmacokinetic parameters of a polypeptide, the Bowman-Birk protease inhibitor (BBI), and its palmitic acid conjugate. *Pharm. Res.* **13**:1373–1377 (1996).
13. J. Wang, D. Shen, and W. C. Shen. Preparation, purification, and characterization of a reversibly lipidized desmopressin with potentiated anti-diuretic activity. *Pharm. Res.* **16**:1674–1679 (1999).
14. J. Wang, D. Chow, H. Heiati, and W. C. Shen. Reversible lipidization for the oral delivery of salmon calcitonin. *J. Control. Rel.* **88**:369–380 (2003).
15. W. A. Murphy, C. A. Meyers, and D. H. Coy. Potent, highly selective inhibition of growth hormone secretion by position 4 somatostatin analogs. *Endocrinology* **109**:491–495 (1981).
16. L. Bokser and A. V. Schally. Delayed release formulation of the somatostatin analog RC-160 inhibits the growth hormone (GH) response to GH-releasing factor-(1-29)NH2 and decreases elevated prolactin levels in rats. *Endocrinology* **123**:1735–1739 (1988).
17. P. J. McConahey and F. J. Dixon. Radioiodination of proteins by the use of the chloramine-T method. *Methods Enzymol.* **70**:210–213 (1980).

18. T. Karashima, R. Z. Cai, and A. V. Schally. Effects of highly potent octapeptide analogs of somatostatin on growth hormone, insulin and glucagon release. *Life Sci.* **41**:1011–1019 (1987).
19. V. J. Hruby. Conformational restrictions of biologically active peptides via amino acid side chain groups. *Life Sci.* **31**:189–199 (1982).
20. S. Siehler, K. Seuwen, and D. Hoyer. [125I][Tyr3]octreotide labels human somatostatin sst2 and sst5 receptors. *Eur. J. Pharmacol.* **348**:311–320 (1998).
21. S. W. Lamberts, J. C. Reubi, W. H. Bakker, and E. P. Krenning. Somatostatin receptor imaging with 123I-Tyr3-Octreotide. *Z. Gastroenterol.* **28**:20–21 (1990).
22. W. H. Bakker, E. P. Krenning, W. A. Breeman, J. W. Koper, P. P. Kooij, J. C. Reubi, J. G. Klijn, T. J. Visser, R. Docter, and S. W. Lamberts. Receptor scintigraphy with a radioiodinated somatostatin analogue: radiolabeling, purification, biologic activity, and in vivo application in animals. *J. Nucl. Med.* **31**:1501–1509 (1990).
23. M. Lemaire, M. Azria, R. Dannecker, P. Marbach, A. Schweitzer, and G. Maurer. Disposition of sandostatin, a new synthetic somatostatin analogue, in rats. *Drug Metab. Dispos.* **17**:699–703 (1989).
24. T. Yamada, Y. Kato, H. Kusuhara, M. Lemaire, and Y. Sugiyama. Characterization of the transport of a cationic octapeptide, octreotide, in rat bile canalicular membrane: possible involvement of P-glycoprotein. *Biol. Pharm. Bull.* **21**:874–878 (1998).
25. G. Fricker, V. Dubost, D. Schwab, C. Bruns, and C. Thiele. Heterogeneity in hepatic transport of somatostatin analog octapeptides. *Hepatology* **20**:191–200 (1994).
26. Z. Kan, P. A. McCuskey, K. C. Wright, and S. Wallace. Role of Kupffer cells in iodized oil embolization. *Invest. Radiol.* **29**:990–993 (1994).
27. N. C. Phillips and M. S. Tsao. Liposomal muramyl dipeptide therapy of experimental M5076 liver metastases in mice. *Cancer Immunol. Immunother.* **33**:85–90 (1991).
28. D. M. Nott, J. Y. Baxter, J. S. Grime, D. W. Day, T. G. Cooke, and S. A. Jenkins. Effects of a somatostatin analogue (SMS 201-995) on the growth and development of hepatic tumour derived by intraportal injection of Walker cells in the rat. *Br. J. Surg.* **76**:1149–1151 (1989).
29. N. Davies, H. Kynaston, J. Yates, B. A. Taylor, and S. A. Jenkins. Octreotide, the reticuloendothelial system, and experimental liver tumour. *Gut* **36**:610–614 (1995).
30. N. Davies, J. Yates, H. Kynaston, B. A. Taylor, and S. A. Jenkins. Effects of octreotide on liver regeneration and tumour growth in the regenerating liver. *J. Gastroenterol. Hepatol.* **12**:47–53 (1997).